Molecular Crystals and Liquid Crystals
Publication details, including instructions for authors and subscription information:
http://www.tandfonline.com/loi/gmcl20

Electroluminescence Generated from ITO/α-NPD/Alq_3/Al Diodes by Applying A.C. Square Voltage

Atsuo Sadakata [a], Tetsuya Yamamoto [a], Dai Taguchi [a], Takaaki Manaka [a], Masahiro Fukuzawa [b] & Mitsumasa Iwamoto [a]

[a] Department of Physical Electronics, Tokyo Institute of Technology, Tokyo, Japan

[b] Department of Electrical Engineering and Information Technology, Kyushu Sangyo University, Fukuoka, Japan

Version of record first published: 17 Sep 2012.

To cite this article: Atsuo Sadakata , Tetsuya Yamamoto , Dai Taguchi , Takaaki Manaka , Masahiro Fukuzawa & Mitsumasa Iwamoto (2012): Electroluminescence Generated from ITO/α-NPD/Alq_3/Al Diodes by Applying A.C. Square Voltage, Molecular Crystals and Liquid Crystals, 567:1, 187-192

To link to this article: http://dx.doi.org/10.1080/15421406.2012.703806

Mol. Cryst. Liq. Cryst., Vol. 567: pp. 187–192, 2012

ISSN: 1542-1406 print/1563-5287 online
DOI: 10.1080/15421406.2012.703806

Taylor & Francis
Taylor & Francis Group

Electroluminescence Generated from ITO/α-NPD/Alq_3/Al Diodes by Applying A.C. Square Voltage

ATSUO SADAKATA,[1] TETSUYA YAMAMOTO,[1] DAI TAGUCHI,[1] TAKAAKI MANAKA,[1] MASAHIRO FUKUZAWA,[2] AND MITSUMASA IWAMOTO[1,*]

[1]Department of Physical Electronics, Tokyo Institute of Technology, Tokyo, Japan
[2]Department of Electrical Engineering and Information Technology, Kyushu Sangyo University, Fukuoka, Japan

We measured the electroluminescence (EL) generated from double-layer ITO/α-NPD/Alq_3/Al diodes by applying large A.C. square voltages for understanding carrier behaviors. Two EL modes were identified in high and low frequency regions, relying on the D.C. component of the applied A.C. square voltages. This indicates that two different carrier behaviors are responsible for the EL emission from the double-layer EL diodes. Modeling the two EL modes, we showed the contribution of the D.C. component of applied A.C. square voltages to the two EL modes in terms of the interfacial Maxwell-Wagner charging.

Keywords Organic light-emitting diodes; Maxwell-Wagner effect; A.C. square voltages; Frequency dependence of electroluminescence

Introduction

Organic light-emitting diodes (OLED) are being used in electronics such as illumination and display devices, and the EL market is expected to be growing year after year. Accordingly, the development of OLED devices that show high performance is demanded. It was the work of Tang's group that marked a breakthrough to the field of electronics [1]. They showed the enhancement of high-intensity EL by using a double-layer OLED device. Since then many experimental and theoretical studies have been carried out, but these are still not sufficient. Before the Tang's work, electroluminescence had drawn much attention in the field of electrical insulation engineering as one of pre-breakdown phenomena of insulators [2, 3]. The EL generated from insulators being stressed under A.C. voltage was very weak, but it was very helpful for diagnosis of insulators used as in power cables. Accordingly techniques for studying carrier behavior have been developed in terms of ELs. Among them is an experimental technique that utilizes large A.C. voltage with D.C. component.

*Address correspondence to Prof. Mitsumasa Iwamoto, Department of Physical Electronics, Tokyo Institute of Technology, 2-12-1 O-okayama, Meguro-ku, Tokyo, 152-8552, Japan. Tel.: (+81)03-5734-2191; Fax: (+81)03-5734-2191. E-mail: iwamoto@pe.titech.ac.jp

In this study, we utilized the large A.C. voltage with D.C. component for understanding carrier behaviors in OLED. That is, our aim of the use of A.C. voltage is to clarify the carrier behavior, and not to show an A.C. driving method for OLED operation with high performance [4]. We measured the frequency dependence of the EL emission from a double-layer OLED device with a structure of ITO/α-NPD/Alq_3/Al by applying A.C. square voltages. In the low frequency region, the EL intensity generated by applying the A.C. square voltage with non-zero D.C. component was low in comparison with that generated by applying the A.C. square voltage with zero D.C. component (1st EL mode). In the middle frequency region, the EL intensity gradually decayed with increasing the frequency of applied A.C. square voltages. In the high frequency region, the EL intensities again increased by applying the A.C. square voltages with non-zero D.C. component (2nd EL mode). By using the Maxwell-Wagner effect model, we explained the EL enhancement in the low and high frequency regions.

Experimental

Figure 1 shows the structure of the OLEDs used here, i.e., ITO/α-NPD/Alq_3/Al. We used the *N,N′*-di-[(1-naphthyl)-*N,N′*-diphenyl]-(1,1′-biphenyl)-4,4′-diamine (α-NPD) as a hole transport layer and the tris(8-hydroxy-quinolinato) aluminum (III) (Alq_3) as an electron transport and light-emitting layer. α-NPD molecules were deposited on a cleaned ITO glass substrate, onto which Alq_3 molecules were deposited by the conventional resistive thermal evaporation method. The thicknesses of the α-NPD and Alq_3 layers were 150 nm and 50 nm, respectively. Finally, aluminum electrode was deposited. All resulting devices were encapsulated in a small vessel with silica-gels and deoxidizers to avoid degradation caused by moisture and oxygen.

Figure 1 shows the experimental setup. We operated the OLED devices by applying an A.C. square voltage with wave forms illustrated in Fig. 1. The frequency region is between 10 Hz and 5 MHz. The plus amplitude of A.C. square voltages V_a was fixed at +20 V, while the minus amplitude V_b was varied between 0 V and −20 V. The duty ratio of the applied A.C. square voltage was 50%, and the applied A.C. square voltage $V(t)$ is given as sum of the D.C. and sinusoidal wave voltages as

$$V(t) = \frac{V_a + V_b}{2} + \sum_{m=1}^{\infty} \left\{ \frac{2(V_a - V_b)}{\pi(2m-1)} \sin \frac{2\pi(2m-1)}{T} t \right\}, \quad (1)$$

with $T(= 1/f; f$: frequency). Applied A.C. square voltages were generated using a function generator (NF, WF1974) and a high speed amplifier (NF, HSA4101). We measured the EL

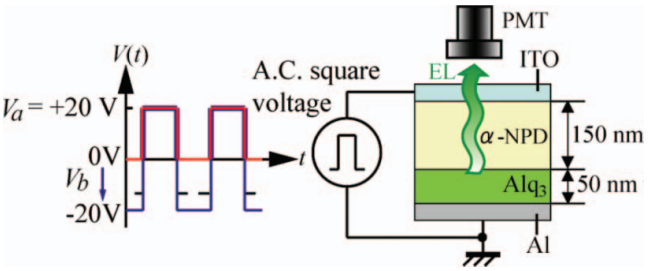

Figure 1. A structure of double-layer OLED (ITO/α-NPD/Alq_3/Al) and the experimental set-up.

intensity emitted from the OLED devices as a function of the frequency of applied A.C. square voltages. The emitted EL light was collected using a photo multiplier tube (PMT: Hamamatsu, R3896) and the EL intensity was measured by an ammeter (Keithley 2000). All experiments were performed in dark.

Results

Figure 2(a) shows the frequency dependence of EL intensities by applying the various waveforms of A.C. square voltages. The waves a and b of the applied A.C. square voltage are denoted in the figure. The first term of Eq. (1) suggests that the D.C. component $(V_a + V_b)/2$ of waves a and b are 0 V and +10 V, respectively (see Fig. 1). That is, the amplitude of D.C. components changes in proportion to the V_b. Results showed that the EL intensities were dependent on the applied A.C. square voltages, as shown in Fig. 2(a). Region 1 is the low frequency region, where the EL intensity is nearly constant, but the EL intensity relies on the D.C. component $V_{dc}(= (V_a + V_b)/2)$, and it decreases with increase of the D.C. component. Region 2 is the intermediate frequency region, where the EL intensity gradually decays with increase of the frequency of applied A.C. square voltages. Region 3 is the high frequency region, where the EL intensity relies on the applied waveform. For wave a with zero-D.C. voltage component, the EL intensity only decreases. On the one hand, for wave b with non-zero positive D.C. component, $V_a/2$, the EL is generated and its intensity increases with the amplitude of D.C. component. Figure 2(b) shows the relationship between the D.C. component voltage V_{dc} and the EL intensity of applied A.C. square voltage at frequency 3 MHz. The EL intensity is enhanced in the region $V_{dc} > 8.4$ V, corresponding to the applied $V_b > -3.2$ V. That is, the generated EL at 3 MHz is governed by the D.C. voltage component.

Discussions

There are two EL modes for the double-layer ITO/α-NPD/Alq$_3$/Al diodes, as seen in Fig. 2(a). The first one appears in the lower frequency region and the second one in the

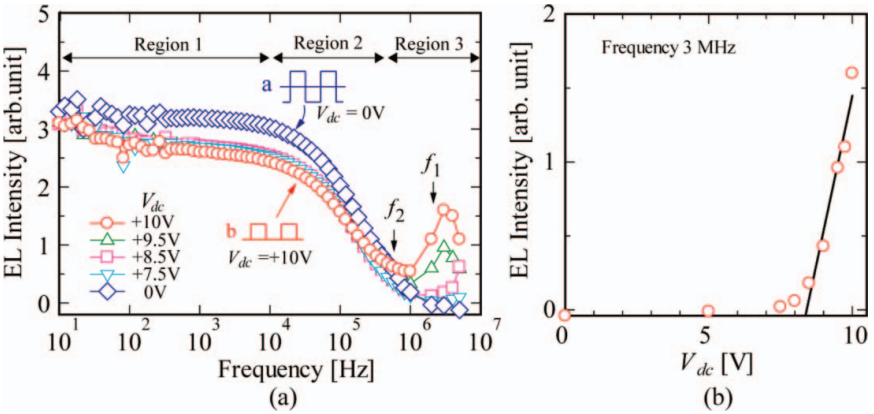

Figure 2. (a) The ELs generated from a double-layer OLED (ITO/α-NPD/ Alq$_3$/Al) as functions of the frequency of applied A.C. square wave voltages. (b) The relationship between the EL intensity and the D.C. component voltage $V_{dc}(= (V_a + V_b)/2)$ of applied A.C. square voltage waveforms at 3 MHz.

high frequency region. The decaying of the EL intensity in the middle frequency region is explained as follows: The carrier transit time across a layer is given as $d/\mu E$, where film thickness d, dielectric constant ε, carrier mobility μ, E is the electric field across the layer. In our experiments, we applied the A.C. square voltages given by Eq. (1) to the devices. That is, the applied D.C. voltage across the double-layer is $V_{ex} = V_a$ or V_b, alternately. Accordingly, the direction of external electric field changes alternately. For $\varepsilon_1 = 3.1$, $\varepsilon_2 = 4.2$, $d_1 = 150$ nm, $d_2 = 50$ nm (1:α-NPD, 2:Alq_3) and $V_{ex} = \pm 20$ V, we obtain the hole and electron transit time $t_1 = 170$ nsec, and $t_2 = 630$ nsec, respectively, assuming that the hole mobility of α-NPD is $\mu_1 = 10^{-4}$ cm^2/Vs and electron mobility of Alq_3 is $\mu_2 = 10^{-5}$ cm^2/Vs [5]. Interestingly, transit times, t_1 and t_2, correspond well with the frequencies that give minimum EL intensity at $f_1 = 1/2t_1$ (= 2.9MHz) and $f_2 = 1/2t_2$ (= 790 kHz) (see Fig. 2(a)), respectively. These results indicate that carrier transits across the Alq_3 and α-NPD layers govern the EL decaying in the middle frequency region.

It is instructive here to note that a current flows during the EL emission from the double-layer ITO/α-NPD/Alq_3/Al diodes. According to the Maxwell-Wagner effect [6–9], excess charge accumulates at the double-layer interface due to the difference of relaxation time $\tau(= \varepsilon/\sigma)$, where ε and σ are dielectric constant and conductivity, respectively. For the ITO/α-NPD/Alq_3/Al diodes, the relaxation times of α-NPD,τ_1, and Alq_3, τ_2 are different, $\tau_1 \neq \tau_2$. Consequently, charge Q_s is accumulated at the interface. By applying the A.C. square voltage $V(t)$ given by Eq. (1), the interfacial charge Q_s is accumulated and a potential $V_s(= Q_s/(C_1 + C_2))$ is built at the α-NPD/Alq_3 interface with reference to the electrodes. Accordingly, the internal electric fields in the α-NPD layer and Alq_3 layer become as follows:

$$E_1 = \frac{C_2}{C_1 + C_2} V_{ex} \frac{1}{d_1} - \frac{Q_s}{C_1 + C_2} \frac{1}{d_1}, \quad E_2 = \frac{C_1}{C_1 + C_2} V_{ex} \frac{1}{d_2} + \frac{Q_s}{C_1 + C_2} \frac{1}{d_2}. \quad (2)$$

Here C_1, C_2, and G_1, G_2 are capacitance and conductance of α-NPD layer and Alq_3 layer, respectively. Equation (2) suggests that the electric field E_1 decreases due to accumulation of positive charge Q_s, while the electric field E_2 increases. The increase of electric field assists carrier transport in the corresponding layer and the carrier transit time decreases accordingly. On the other hand, the decrease of electric field suppresses the carrier transport and the carrier transit time increases accordingly. Significant effect also appears in the carrier injection due to the presence of interfacial charge Q_s. That is, the interfacial charge Q_s contributes to assist and suppress the carrier injection, relying on the polarity and amount of accumulated charge (see Eq. (2)).

In the lower frequency region, the 1st EL is activated. In this region holes and electrons inject from the opposite electrodes, and they recombine at the α-NPD/Alq_3 interface, during the +20 V cycle of applied A.C. square voltages, because holes and electrons can transit across the α-NPD and Alq_3 layers, respectively. The interfacial charge Q_s is accumulated due to the Maxwell-Wagner effect, and a potential V_s is created at the α-NPD/Alq_3 interface. As a result, the electric field of α-NPD decreases according to the Eq. (2), and the hole injection from the ITO electrode is suppressed. These result in the decrease of the EL intensity, and the EL intensity decreases with increase of the D.C. component of the applied A.C. square voltage in the low frequency region of Fig. 2(a).

In the higher frequency region, the 2nd EL is activated. In this region, injected electrons from the Al electrode cannot catch up the alternating applied A.C. square voltage. Accordingly, the Maxwell-Wagner type interfacial charge Q_s at the α-NPD/Alq_3 interface makes a dominant contribution. Figure 3(a) depicts a model under short circuit condition,

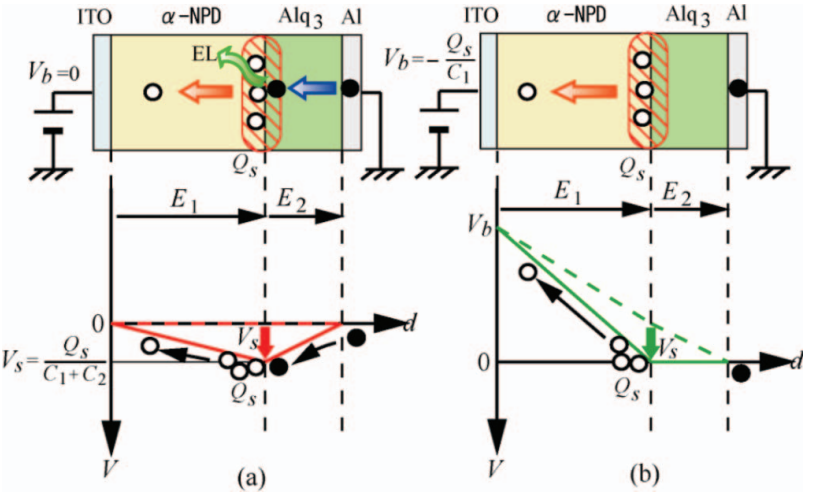

Figure 3. Model of carrier behaviors and potential profiles in double-layer OLED devices. (a) Carrier behaviors and a potential profile under short circuit condition $V_{ex} = 0$ V. Accumulated charge Q_s generates a potential V_s at the interface. (b) Carrier behaviors and a potential profile that the 2nd EL mode cannot generate. Broken lines in the potential profiles represent the internal potential of α-NPD and Alq_3 by applying the voltage V_{ex} with $Q_s = 0$. Solid lines represent the modulated internal potential of α-NPD and Alq_3 by internal potential $V_s(= Q_s/(C_1 + C_2))$ with $Q_s > 0$.

in the presence of accumulated positive charge Q_s at the interface. A potential V_s is built at the interface, and results in space charge fields of α-NPD $E_1 = -V_s/d_1$, and of Alq_3 $E_2 = V_s/d_2$. Consequently, accumulated positive charge Q_s gradually leaves from the interface to the ITO electrode by the electric field E_1, whilst electrons are injected from the Al electrode and supplied to the α-NPD/Alq_3 interface. Accordingly, the EL emission is allowed due to the recombination of accumulated holes Q_s with electrons supplied from the Al electrode. Using this model, the change of the 2nd EL intensity, in proportion to the D.C. voltage component of applied A.C. square voltages, is acceptable under the condition of $E_2 > 0$, because accumulated charge Q_s is proportional to the current flowing through the device by the D.C. component of applied A.C. square voltages. Note that the 2nd EL is not generated when the electric field $E_2 < 0$, i,.e., the potential $V_b = -Q_s/C_1$ (see Fig. 3(b)), and this well accounts for the result of Fig. 2(b).

Conclusion

We studied the EL emission from the double-layer OLED device with structure of ITO/α-NPD/Alq_3/Al by applying A.C. square voltages. Results showed the presence of two EL modes, and these are activated at low and high frequency regions, depending on the D.C. voltage component of applied A.C. square voltages, where the interfacial charge Q_s accumulated due to the Maxwell-Wagner effect makes a significant contribution.

References

[1] Tang, C. W., & Van Slyke, S. A. (1987). *Appl. Phys. Lett.*, *51*, 913.
[2] Hartman, W. A., & Armstrong, H. L. (1967). *J. Appl. Phys.*, *38*, 2393.
[3] Bamji, S. S. (1999). *IEEE Electr. Insul. Mag.*, *15*, 9.

[4] For example, Cusumano, P., Buttitta, F., Di Cristofalo, A., & Cali, C. (2003). *Synth. Met.*, *139*, 661; Wang, Y. Z., Gebler, D. D., Lin, L. B., Blatchford, J. W., Wang, H. L., Epstein, A. J., & Jessen, S. W. (1996). *Appl. Phys. Lett.*, *68*, 894; Zou, D., Yahiro, M., & Tsutsui, T. (1998). *Jpn. J. Appl. Phys.*, *37*, L1406.
[5] Naka, S., Okada, H., Onnagawa, H., Yamaguchi, Y., & Tsutsui, T. (2000). *Synth. Met.*, *111–112*, 331.
[6] Maxwell, J. C. (1954). *A Treatise on Electricity & Magnetism,* Vol. 1, Chapter X, pp. 450–464, Dover: New York.
[7] Oka, S. & Nakata, O. (1960). *Kotai Yudentai Ron*, Chapter 5, pp. 80–105, Iwanami: Tokyo.
[8] Taguchi, D., Weis, M., Manaka, T., & Iwamoto, M. (2009). *Appl. Phys. Lett.*, *95*, 263310.
[9] Taguchi, D., Inoue, S., Zhang, L., Li, J., Weis, M., Manaka, T., & Iwamoto, M. (2010). *J. Phys. Chem. Lett.*, *1*, 803.